Hindawi Publishing Corporation
EURASIP Journal on Wireless Communications and Networking
Volume 2009, Article ID 367097, 11 pages
doi:10.1155/2009/367097

Research Article

M-PSK Cooperative Trellis Codes for Coordinate Interleaved Coded Cooperation

Özgür Oruç and Ümit Aygölü

Faculty of Electrical and Electronics Engineering, Istanbul Technical University, Maslak, 34469 Istanbul, Turkey

Correspondence should be addressed to Ümit Aygölü, aygolu@itu.edu.tr

Received 31 October 2008; Revised 2 March 2009; Accepted 29 May 2009

Recommended by Xavier Mestre

M-PSK cooperative trellis codes are proposed for two-user coordinate interleaved coded cooperation operating over quasistatic Rayleigh fading channels. The coding approach properly combines cooperative and modulation diversity techniques to take their full advantage. Two selective cooperation schemes are considered related to whether users know the cooperation status or not. Upper bounds on the pairwise error probability of the considered schemes are derived for each cooperation case which lead to new code design criteria. Based on these criteria, 4-, 8-, 16-state QPSK and 8-, 16-state 8PSK cooperative trellis codes are obtained by means of exhaustive computer search. The error performance evaluation of the new codes by computer simulations shows that they outperform the corresponding best space-time codes used in cooperation with coordinate interleaving.

1. Introduction

Spatial diversity techniques are extensively used to enhance wireless system performance against deterioration caused by fading, since it needs neither extra transmission time nor bandwidth expansion. The link performance is enhanced by conveying the information signal to the destination over more than one ideally independent fading signal paths in space, time, or frequency, through the use of a transmit antenna array. Although this is a reasonable approach for the base station, it may be impractical for the mobile unit due to the size or cost limitations which prevent the use of multiple antennas. To overcome this problem, cooperative communication is proposed with various aspects in[1–3]. In general, users with single antenna share their antennas which form a virtual antenna array. Each user transmits its own signals to both the destination and the partner(s). Each partner retransmits the received or some version of these signals to the destination to provide spatial diversity in a distributed fashion by means of a virtual multiple antennas transmission. The main difficulty compared to the classical spatial diversity is that the user-to-partner (interuser) channel is noisy and the cooperation system should be designed by taking into account that the received information by the partner may be erroneous. However, it is shown that the cooperation improves the robustness of the wireless system against fading and allows higher data rates.

Two main cooperation methods are amplify-and-forward (AF) and decode-and-forward (DF). In AF [2], cooperating user receives the noisy signal from its partner and retransmits it after amplification. Signals from the user and its partner are combined at the destination to determine transmitted data bits. In DF [2], the cooperating user decodes the signal received from its partner before retransmitting using the same code. Both of these methods guarantee full diversity for two-user case when the interuser channel fading coefficients are known at the destination. It is shown that they increase the channel capacity and improve the system performance in terms of outage probability. However, these schemes can be interpreted as an instance of the repetition coding and therefore bandwidth inefficient. A different approach combining classical channel coding with cooperative diversity is the coded cooperation [3, 4] where instead of repeating the same codeword, the partner provides an additional redundancy to the coding scheme of the user it cooperates. Dividing the codeword of each user into two parts, the first part is transmitted by the user itself and second part by its partner after an error detection to avoid

error propagation which becomes serious when the interuser signal-to-noise ratio (SNR) is low. When a user erroneously detects the first part of its partner's codeword, the second part of its own codeword will be transmitted. Recently, coded cooperation schemes have attracted attention in literature. In [5], a coded user-cooperation scheme based on the turbo encoding/decoding is proposed. Li and Stefanov proposed cooperative multiple trellis coded modulation using asymmetric constellations and compared their codes with repetition-based cooperation techniques in [6, 7].

On the other hand, coordinates of the modulated symbols are affected from independent fading coefficients when they are suitably interleaved before transmission. In literature, this kind of diversity and the corresponding interleaving method were named "modulation diversity" and "coordinate interleaving" (CI) [8, 9], respectively. (We use the abbreviation CI for both "coordinate interleaving" and "coordinate interleaved" in this manuscript.) For multidimensional modulation schemes, achievable diversity order is the minimum number of distinct coordinates of distinct symbol pairs in the constellation. For classical M-PSK, real or imaginary parts of any distinct symbol pair can take the same value which reduce the modulation diversity order to one. However, with suitably rotated M-PSK constellations, both coordinates of distinct symbol pairs become different, thus the maximum modulation diversity order of two is achieved. CI has been used to obtain single symbol decodable space-time block code designs [10], and their distributed applications for relay networks are given in [11]. However, CI trellis code design has not been considered for cooperative systems.

In this paper, we propose two coordinate interleaved coded cooperation (CICC) schemes based on suitable combination of the modulation and cooperative diversity techniques related to whether users know the cooperation case or not. We derive upper bounds on the pairwise error probability (PEP) of the new schemes for each cooperation case and obtain code design criteria based on these upper bounds. 4-, 8-, 16-state QPSK and 8-, 16-state 8PSK cooperative trellis codes which significantly improve the system error performance compared to the corresponding best space-time trellis codes [12] used in cooperation with CI, are proposed. The new codes have 50% cooperation rate, 2/4 and 3/6 generic coding rates for QPSK and 8PSK, respectively. It is shown by computer simulations that 0.5–4.5 dB savings in SNR at a frame error rate of 10^{-3} are possible with the proposed codes.

The rest of the paper is organized as follows. In the next section, the signaling model and CICC schemes are presented. PEP upper bounds are derived in Section 3. New code design criteria and cooperative trellis codes are given in Section 4. Performance results are discussed in Section 5, and finally Section 6 concludes the paper.

2. System Model

2.1. Preliminaries for Cooperative System Model. The considered cooperative system model is shown in Figure 1 where two cooperating users U_1 and U_2 transmit each a sequence of symbols to the same destination D. Transmission from one-antenna users is performed through their own access channel which is part of one of the orthogonal multiple access schemes like TDMA, FDMA, or CDMA.

In classical coded cooperation schemes [4], each user transmits N coded bits corresponding to K information bits which include Cyclic Redundancy Check (CRC) bits. N output bits are divided into two parts, first one formed by unpunctured N_1 bits and the second by punctured N_2 bits where $N = N_1 + N_2$, N_2/N is the cooperation ratio. When the unpunctured N_1 bits are transmitted, each user detects its partner's information bits, checks for the CRC bits, and decides if they are correct or not. If a user correctly decides its partner's information bits during the first part, it cooperates by transmitting N_2 bits of its partner during the second part. Otherwise it does not cooperate and transmits its own punctured N_2 bits. In the coded cooperation scheme given in [4] only a rate 1/4 convolutional code with BPSK modulation is considered for slow fading.

In this paper, we extend the system model to higher-order modulation and introduce coordinate interleaver to the system, to increase both bandwidth efficiency and diversity gain. Coded bits at the users are produced from CRC added information bits by means of a trellis coded modulation scheme where coded bits should be transmitted by mapping to θ^o rotated M-PSK symbols to achieve maximum modulation diversity order. The mapping rule is given in Figure 2 for QPSK and 8PSK constellations.According to the desired cooperation ratio, users divide their transmissions into two parts as similar to the classical coded cooperation. Let $T_{f,1}$ and $T_{f,2}$ denote the time intervals of the fth frame, $T_{f,2}/T_f$ being the cooperation ratio where $T_f = T_{f,1} + T_{f,2}$, since the cooperation is realized in $T_{f,2}$. For a transmission from U_i ($i \in \{1,2\}$) during $T_{f,t}$ ($t \in \{1,2\}$), the received signal sequence at unit $j \in \{1,2,D\}$ can be written as

$$\mathbf{r}_{f,t}^{(ij)} = h_{f,ij}\mathbf{s}_{f,t}^{(i)} + \mathbf{n}_{f,t}^{(ij)}, \tag{1}$$

where $\mathbf{s}_{f,t}^{(i)}$ is the transmitted symbol sequence according to the CICC schemes which will be presented in the next section, $h_{f,ij}$ is the zero-mean complex Gaussian fading coefficients with variance 1/2 in each dimension and $\mathbf{n}_{f,t}^{(ij)}$ is the AWGN sequence whose zero-mean complex components have variance $N_0/2$ in each dimension. All complex fading coefficients are assumed constant during one frame interval and changing independently from one frame to another. The interuser and user-to-destination channels are assumed independent of each other. All receivers perfectly know channel fading coefficients, and the interuser channel is assumed reciprocal, that is, $h_{f,12} = h_{f,21}$. In the sequel, $(\cdot)^*$, $(\cdot)^T$, and $|\cdot|$ denote transpose conjugate, transpose, and the Euclidean norm, respectively.

2.2. CICC Schemes. In a quasistatic fading channel, CI can be performed between symbols of two consecutive frames to form the CI symbol sequences since modulation diversity [9] is provided when real and imaginary parts of each symbol are affected from independent fading coefficients. Therefore, considered transmission schemes will be explained over the

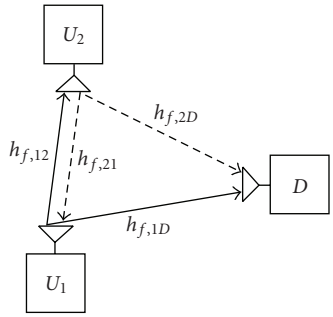

Figure 1: Cooperative system model.

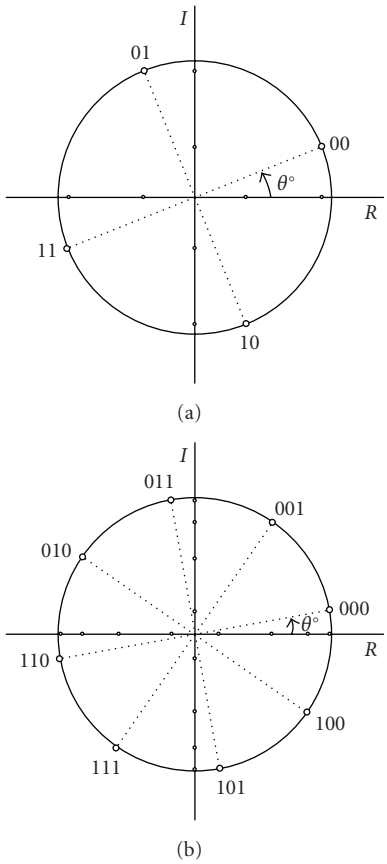

Figure 2: θ^o rotated (a) QPSK and (b) 8PSK symbols and corresponding bit mappings.

first and second frames, and for simplicity, the decoding processes will be derived for U_1, in the sequel.

The coded symbol sequence and its CI version for U_i at the fth frame are denoted by $\mathbf{x}_f^{(i)}$ and $\tilde{\mathbf{x}}_f^{(i)}$, respectively, where $f \in \{1,2\}$. Coordinate interleaving process is performed by $\tilde{\mathbf{x}}_1^{(i)} = \mathbf{x}_{1R}^{(i)} + j\mathbf{x}_{2I}^{(i)}$ and $\tilde{\mathbf{x}}_2^{(i)} = \mathbf{x}_{2R}^{(i)} + j\mathbf{x}_{1I}^{(i)}$, where $\mathbf{x}_{fR}^{(i)}$ and $\mathbf{x}_{fI}^{(i)}$ denote real and imaginary parts of the coded symbol sequence $\mathbf{x}_f^{(i)}$, respectively. Users divide their symbol sequences $\mathbf{x}_f^{(i)}$ into unpunctured $\mathbf{x}_f^{(i)u}$ and punctured $\mathbf{x}_f^{(i)p}$ symbol sequences according to the desired cooperation ratio. CI versions of $\mathbf{x}_f^{(i)u}$ and $\mathbf{x}_f^{(i)p}$ are denoted by $\tilde{\mathbf{x}}_f^{(i)u}$ and $\tilde{\mathbf{x}}_f^{(i)p}$, respectively.

Two CICC schemes (Schemes A and B) are considered related to the cooperation status unknown or known at the users. The signaling models for Schemes A and B are given in Figures 3 and 4, respectively. Users send CI symbols $\tilde{\mathbf{x}}_1^{(i)u}$ during $T_{1,1}$ which contain information of the first and second frames. Each symbol can be detected from only its real or imaginary part since, due to the rotation of the signal set, both real and imaginary parts of the symbols are different (Figure 2). Therefore, users can detect information bits of the first and second frames based only on the transmission during $T_{1,1}$ and decide to cooperate when the CRC bits are correctly decoded for both frames. Otherwise, they do not cooperate and send their own punctured symbol sequences. U_1 and U_2 detect each other's information bits of the first and second frames from $\mathbf{x}_{1R}^{(i)u}$ and $\mathbf{x}_{2I}^{(i)u}$ transmitted during $T_{1,1}$. At the end of the time interval $T_{1,1}$, symbol sequence transmitted from U_1 is obtained at U_2 as

$$\mathbf{r}_{1,1}^{(12)} = h_{1,12}\mathbf{s}_{1,1}^{(1)} + \mathbf{n}_{1,1}^{(12)}, \tag{2}$$

where $\mathbf{s}_{1,1}^{(1)} = \tilde{\mathbf{x}}_1^{(1)u} = \mathbf{x}_{1R}^{(1)u} + j\mathbf{x}_{2I}^{(1)u}$. The following theorem simplify the metric calculations at the receivers.

Theorem 1. *Without deinterleaving process, the symbol sequences $\mathbf{x}_{1R}^{(1)u}$ and $\mathbf{x}_{2I}^{(1)u}$ can be separately detected from*

$$\begin{aligned}\hat{\mathbf{x}}_{1R}^{(1)u} &= \arg\min_{\mathbf{x}_{1R}^{(1)u}} \left|\mathbf{r}_{1,1}^{(12)} - h_{1,12}\mathbf{x}_{1R}^{(1)u}\right|^2,\\ \hat{\mathbf{x}}_{2I}^{(1)u} &= \arg\min_{\mathbf{x}_{2I}^{(1)u}} \left|\mathbf{r}_{1,1}^{(12)} - jh_{1,12}\mathbf{x}_{2I}^{(1)u}\right|^2,\end{aligned} \tag{3}$$

where minimizations are over all possible values of $\mathbf{x}_{1R}^{(1)u}$ and $\mathbf{x}_{2I}^{(1)u}$, respectively.

The proof of this theorem is given in the appendix. Note that, the number of sequences to be considered during the minimizations in (3) is reduced using the Viterbi algorithm.

If $\mathbf{x}_{1R}^{(1)u}$ and $\mathbf{x}_{2I}^{(1)u}$ are correctly decided by checking the CRC bits, that is, $\hat{\mathbf{x}}_{1R}^{(1)u} = \mathbf{x}_{1R}^{(1)u}$ and $\hat{\mathbf{x}}_{2I}^{(1)u} = \mathbf{x}_{2I}^{(1)u}$, U_2 transmits the punctured CI symbol sequences of U_1 in $T_{1,2}$ and $T_{2,2}$ according to the cooperation schemes. Otherwise, U_2 transmits its own punctured CI symbols. Same procedure is applied for U_1. Note that during $T_{2,1}$ users send their own unpunctured CI symbols $\tilde{\mathbf{x}}_2^{(i)u}$.

According to the users' decisions to cooperate or not, four different cooperation cases occur. These cases are labeled as C1 (both users cooperate), C2 (both users do not cooperate), C3 (U_1 cooperates, U_2 does not), and C4 (U_2 cooperates, U_1 does not) in Figures 3 and 4. Users send a cooperation flag bit to broadcast cooperation status at the beginning of $T_{1,2}$.

In C3 and C4 of Scheme A, punctured symbol sequence of one user is never transmitted which degrades its error

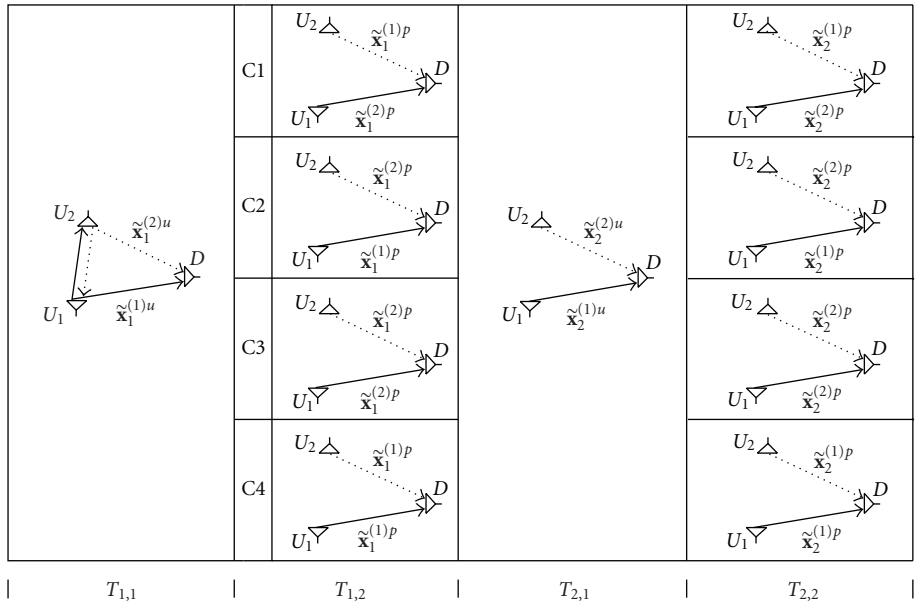

Figure 3: Scheme A: users do not know if the other cooperates or not.

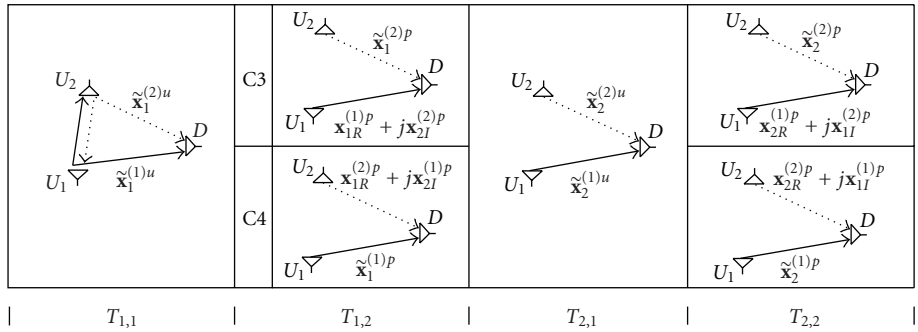

Figure 4: Scheme B: users know if the other cooperates or not.

performance. To overcome this problem, C3 and C4 are modified as in Figure 4 assuming that each user knows if the other cooperates or not by detecting the cooperation flag bit. In these cases, cooperation is performed only at the imaginary part of the symbols and each user sends its own punctured symbols, at the real part. We call this modified scheme as Scheme B, C1, and C2 cases remaining the same for both schemes.

It is assumed that the destination always knows which cooperation case is realized by detecting the cooperation flag bit. Therefore, the transmitted data from U_1 and U_2 during the first and second frames can be detected using appropriate decoding metrics for each cooperation case. If the decision metric for unpunctured symbols of U_1 in the first frame is defined as

$$m_1^{(1)u} = \left|\mathbf{r}_{1,1}^{(1D)} - h_{1,1D}\mathbf{x}_{1R}^{(1)u}\right|^2 + \left|\mathbf{r}_{2,1}^{(1D)} - jh_{2,1D}\mathbf{x}_{1I}^{(1)u}\right|^2, \tag{4}$$

decision metrics for the symbols of U_1 in the first frame are expressed as

$$\begin{aligned}
\text{C1:}\quad & m_1^{(1)} = m_1^{(1)u} + \left|\mathbf{r}_{1,2}^{(2D)} - h_{1,2D}\mathbf{x}_{1R}^{(1)p}\right|^2 \\
& \qquad + \left|\mathbf{r}_{2,2}^{(2D)} - jh_{2,2D}\mathbf{x}_{1I}^{(1)p}\right|^2, \\
\text{C2:}\quad & m_1^{(1)} = m_1^{(1)u} + \left|\mathbf{r}_{1,2}^{(1D)} - h_{1,1D}\mathbf{x}_{1R}^{(1)p}\right|^2 \\
& \qquad + \left|\mathbf{r}_{2,2}^{(1D)} - jh_{2,1D}\mathbf{x}_{1I}^{(1)p}\right|^2, \\
\text{C3:}\quad & m_1^{(1)} = m_1^{(1)u}, \\
\text{C4:}\quad & m_1^{(1)} = m_1^{(1)u} + \left|\mathbf{r}_{1,2}^{(2D)} - h_{1,2D}\mathbf{x}_{1R}^{(1)p}\right|^2 \\
& \qquad + \left|\mathbf{r}_{2,2}^{(2D)} - jh_{2,2D}\mathbf{x}_{1I}^{(1)p}\right|^2 + \left|\mathbf{r}_{1,2}^{(1D)} - h_{1,1D}\mathbf{x}_{1R}^{(1)p}\right|^2 \\
& \qquad + \left|\mathbf{r}_{2,2}^{(1D)} - jh_{2,1D}\mathbf{x}_{1I}^{(1)p}\right|^2
\end{aligned} \tag{5}$$

according to each cooperation case of Scheme A. For the cases C3 and C4 of Scheme B, decision metrics at the destination are modified as follows:

$$\text{C3:}\quad m_1^{(1)} = m_1^{(1)u} + \left|\mathbf{r}_{1,2}^{(1D)} - h_{1,1D}\mathbf{x}_{1R}^{(1)p}\right|^2,$$

$$\text{C4:}\quad m_1^{(1)} = m_1^{(1)u} + \left|\mathbf{r}_{2,2}^{(2D)} - jh_{2,2D}\mathbf{x}_{1I}^{(1)p}\right|^2 + \left|\mathbf{r}_{1,2}^{(1D)} - h_{1,1D}\mathbf{x}_{1R}^{(1)p}\right|^2 + \left|\mathbf{r}_{2,2}^{(1D)} - jh_{2,1D}\mathbf{x}_{1I}^{(1)p}\right|^2. \tag{6}$$

3. Performance Analysis

Without loss of generality, we consider the transmission of U_1 for the performance evaluation and drop the superscript (1) in the sequel.

3.1. Pairwise Error Probability (PEP) Preliminaries. Let the erroneously detected symbol sequence at the receiver side (partner or destination) be $\mathbf{y}_f$ when $\mathbf{x}_f$ is transmitted, then the conditional PEP can be expressed as

$$P\left(\mathbf{x}_f \longrightarrow \mathbf{y}_f \mid \mathbf{h}\right) = Q\left(\sqrt{\frac{D_{\mathbf{h}}^2\left(\mathbf{x}_f, \mathbf{y}_f\right)E_s}{2N_0}}\right), \tag{7}$$

where $\mathbf{h}$ is the channel coefficients vector, E_s is the average symbol energy, N_0 is the complex AWGN variance, $Q(\cdot)$ is Gaussian Q-function, and $D_{\mathbf{h}}^2(\mathbf{x}_f, \mathbf{y}_f)$ is the weighted squared Euclidean distance between $\mathbf{x}_f$ and $\mathbf{y}_f$. Using the inequality $Q(x) \leq (1/2)e^{-x^2/2}$, (7) is upper bounded as

$$P\left(\mathbf{x}_f \longrightarrow \mathbf{y}_f \mid \mathbf{h}\right) \leq \frac{1}{2}\exp\left(-\gamma D_{\mathbf{h}}^2\left(\mathbf{x}_f, \mathbf{y}_f\right)\right), \tag{8}$$

where $\gamma = E_s/4N_0$. Assuming that $\mathbf{x}_f$ and $\mathbf{y}_f$ are row vectors, the squared Euclidean distance between unpunctured and punctured real parts of $\mathbf{x}_f$ and $\mathbf{y}_f$ are expressed as (The superscript 2 denoting the square is omitted for d_{fR}^u, d_{fR}^p, and d_{fR}^τ to avoid notation complexity.)

$$d_{fR}^u = \left(\mathbf{x}_{fR}^u - \mathbf{y}_{fR}^u\right)\left(\mathbf{x}_{fR}^u - \mathbf{y}_{fR}^u\right)^T, \tag{9}$$

$$d_{fR}^p = \left(\mathbf{x}_{fR}^p - \mathbf{y}_{fR}^p\right)\left(\mathbf{x}_{fR}^p - \mathbf{y}_{fR}^p\right)^T, \tag{10}$$

respectively. The total squared Euclidean distance for real components is calculated from

$$d_{fR}^\tau = d_{fR}^u + d_{fR}^p = \left(\mathbf{x}_{fR} - \mathbf{y}_{fR}\right)\left(\mathbf{x}_{fR} - \mathbf{y}_{fR}\right)^T. \tag{11}$$

Squared Euclidean distances, for the imaginary parts, can be expressed similar to (9)–(11).

3.2. PEP Upper Bounds for Decisions at the Users. Interuser channel performance is dependent on decoding process at the users. Using the decoding metrics applied at the users in $T_{1,1}$ given by (3), the weighted squared Euclidean distances used in (7) for the first and second frames are given as

$$D_{\mathbf{h}}^2(\mathbf{x}_1, \mathbf{y}_1) = d_{1R}^u \left|h_{1,12}\right|^2, \tag{12}$$

$$D_{\mathbf{h}}^2(\mathbf{x}_2, \mathbf{y}_2) = d_{2I}^u \left|h_{2,12}\right|^2, \tag{13}$$

respectively. By taking the expectation of (8) over $\mathbf{h} = [h_{1,12}, h_{2,12}]$, upper bounds on PEP for $\mathbf{x}_1$ and $\mathbf{x}_2$ are obtained as

$$P(\mathbf{x}_1 \longrightarrow \mathbf{y}_1) \leq \frac{1}{2}\left(\frac{1}{1 + d_{1R}^u\gamma}\right), \tag{14}$$

$$P(\mathbf{x}_2 \longrightarrow \mathbf{y}_2) \leq \frac{1}{2}\left(\frac{1}{1 + d_{2I}^u\gamma}\right), \tag{15}$$

respectively. Therefore, the minimum values of d_{1R}^u and d_{2I}^u over all $(\mathbf{x}_1, \mathbf{y}_1)$ and $(\mathbf{x}_2, \mathbf{y}_2)$ pairs have to be maximized to increase the interuser channel performance.

3.3. PEP Upper Bounds for Decisions at the Destination. For the four cooperation cases of Scheme A, the weighted squared Euclidean distances in (7) are expressed as follows:

$$\begin{aligned}
&\text{C1:}\quad D_{\mathbf{h}}^2(\mathbf{x}_1, \mathbf{y}_1) = d_{1R}^u \left|h_{1,1D}\right|^2 + d_{1I}^u \left|h_{2,1D}\right|^2 + d_{1R}^p \left|h_{1,2D}\right|^2 + d_{1I}^p \left|h_{2,2D}\right|^2,\\
&\text{C2:}\quad D_{\mathbf{h}}^2(\mathbf{x}_1, \mathbf{y}_1) = d_{1R}^\tau \left|h_{1,1D}\right|^2 + d_{1I}^\tau \left|h_{2,1D}\right|^2,\\
&\text{C3:}\quad D_{\mathbf{h}}^2(\mathbf{x}_1, \mathbf{y}_1) = d_{1R}^u \left|h_{1,1D}\right|^2 + d_{1I}^u \left|h_{2,1D}\right|^2,\\
&\text{C4:}\quad D_{\mathbf{h}}^2(\mathbf{x}_1, \mathbf{y}_1) = d_{1R}^\tau \left|h_{1,1D}\right|^2 + d_{1I}^\tau \left|h_{2,1D}\right|^2 + d_{1R}^p \left|h_{1,2D}\right|^2 + d_{1I}^p \left|h_{2,2D}\right|^2.
\end{aligned} \tag{16}$$

By taking the expectation of (7) over $\mathbf{h} = [h_{1,1D}, h_{1,2D}, h_{2,1D}, h_{2,2D}]$, PEP upper bounds for each cooperation case are obtained as follows:

$$\begin{aligned}
&\text{C1:}\quad P(\mathbf{x}_1 \longrightarrow \mathbf{y}_1) \leq \frac{1}{2}\left(\frac{1}{1+d_{1R}^u\gamma}\right)\left(\frac{1}{1+d_{1I}^u\gamma}\right)\left(\frac{1}{1+d_{1R}^p\gamma}\right)\left(\frac{1}{1+d_{1I}^p\gamma}\right),\\
&\text{C2:}\quad P(\mathbf{x}_1 \longrightarrow \mathbf{y}_1) \leq \frac{1}{2}\left(\frac{1}{1+d_{1R}^\tau\gamma}\right)\left(\frac{1}{1+d_{1I}^\tau\gamma}\right),\\
&\text{C3:}\quad P(\mathbf{x}_1 \longrightarrow \mathbf{y}_1) \leq \frac{1}{2}\left(\frac{1}{1+d_{1R}^u\gamma}\right)\left(\frac{1}{1+d_{1I}^u\gamma}\right),\\
&\text{C4:}\quad P(\mathbf{x}_1 \longrightarrow \mathbf{y}_1) \leq \frac{1}{2}\left(\frac{1}{1+d_{1R}^\tau\gamma}\right)\left(\frac{1}{1+d_{1I}^\tau\gamma}\right)\left(\frac{1}{1+d_{1R}^p\gamma}\right)\left(\frac{1}{1+d_{1I}^p\gamma}\right).
\end{aligned} \tag{17}$$

Considering Scheme B, the weighted squared Euclidean distances and upper bounds on PEP for cases C3 and C4 are modified, respectively, as follows:

$$\text{C3:}\quad D_{\mathbf{h}}^2(\mathbf{x}_1,\mathbf{y}_1) = d_{1R}^{\tau}\,|h_{1,1D}|^2 + d_{1I}^{u}\,|h_{2,1D}|^2$$

$$P(\mathbf{x}_1 \longrightarrow \mathbf{y}_1) \le \frac{1}{2}\left(\frac{1}{1+d_{1R}^{\tau}\gamma}\right)\left(\frac{1}{1+d_{1I}^{u}\gamma}\right),$$

$$\text{C4:}\quad D_{\mathbf{h}}^2(\mathbf{x}_1,\mathbf{y}_1) = d_{1R}^{\tau}\,|h_{1,1D}|^2 + d_{1I}^{\tau}\,|h_{2,1D}|^2 + d_{1I}^{p}\,|h_{2,2D}|^2$$

$$P(\mathbf{x}_1 \longrightarrow \mathbf{y}_1) \le \frac{1}{2}\left(\frac{1}{1+d_{1R}^{\tau}\gamma}\right)\left(\frac{1}{1+d_{1I}^{\tau}\gamma}\right)\left(\frac{1}{1+d_{1I}^{p}\gamma}\right) \tag{18}$$

upper bounds for the other cases remaining same as given in (17). Note that the PEP upper bounds for the other frames can be similarly written as (17) and (18).

For $\gamma \gg 1$, upper bounds on PEP for all cases in both schemes are approximated by

$$P(\mathbf{x}_1 \longrightarrow \mathbf{y}_1) \le \frac{1}{2}\gamma^{-\eta}\prod_{(q,w)\in\rho}\left(d_{1q}^{w}\right)^{-1}, \tag{19}$$

where the set ρ is the set of all (q,w) pairs where $q \in \{R,I\}$, $w \in \{u,p,\tau\}$ and for which $d_{1q}^{w} \neq 0$, and η is the cardinality of ρ. In (19), the upper bound on PEP is inversely proportional to γ^{η}, and thus the diversity order is η. If $d_{1q}^{w} \neq 0$ for all (q,w) pairs of (17), maximum diversity order of four is achieved for both users when both of them successfully decode each others and cooperate (C1). The diversity order is doubled compared to the nocooperation case (C2), where diversity order is limited to two coming from CI. In (19), a coding advantage of $\prod_{(q,w)\in\rho}(d_{1q}^{w})$ is also achieved.

4. New Code Design Criteria and Cooperative Trellis Codes

4.1. New Code Design Criteria for CICC. From PEP upper bounds for CICC schemes given in Figures 3 and 4, maximum achievable diversity order is four which can be achieved by proper coding in high SNR region. Both users are able to hold this desired diversity order for the case C1. Therefore, the realization percentages of C1 have to be maximized at first. This is our first design criterion which we call *cooperation criterion* since both users cooperate in C1. Maximum diversity order of four is achieved when all squared Euclidean distances related to the PEP upper bound for C1 differ from zero. This is our second design criterion which corresponds to *diversity*. Finally, coding gain of the new codes should be maximized to reach minimum error probability. This is our third and last design criterion named as *the coding advantage*.

Code design criteria for CICC can be summarized as follows.

(1) *Cooperation Criterion.* To achieve the full cooperation case (C1) with maximum percentage of realization, the minimum values of d_{fR}^{u} and d_{fI}^{u} have to be maximized.

(2) *Diversity Criterion.* To achieve the maximum diversity order of four for C1, d_{fR}^{u}, d_{fI}^{u}, d_{fR}^{p}, and d_{fI}^{p} values have to be nonzero.

(3) *Coding Advantage Criterion.* To achieve maximum coding advantage for C1, the minimum value of the product $d_{fR}^{u}d_{fI}^{u}d_{fR}^{p}d_{fI}^{p}$ has to be maximized over all distinct symbol sequences.

Note that the cooperation criterion is related to interuser channel performance, the two others to user-to-destination channel performance.

4.2. Cooperative Trellis Encoder Structure and New Codes (NC). The generic rate k/n cooperative trellis encoder used in the exhaustive code search is shown in Figure 5, where b_{μ}^{ξ}, c^{ζ}, and $g_{\mu,\zeta}^{\xi}$ are the μth information content of the ξth shift register, ζth coded bit and μth binary multiplication coefficient of the ξth shift register and the ζth coded bit, respectively, ($\xi = 1,2,\ldots,k$, $\zeta = 1,2,\ldots,n$, $\mu = 0,1,2,\ldots,\upsilon_{\xi}$). Here υ_{ξ} is the memory order of the ξth shift register. The total memory order of the encoder, denoted by υ, is obtained from $\upsilon = \sum_{\xi=1}^{k}\upsilon_{\xi}$. The total number of states for the trellis encoder is 2^{υ}. Multiplier outputs from all shift registers are added by modulo two, giving the encoder output. The encoder output for ζth coded bit can be computed as $c^{\zeta} = \sum_{\xi=1}^{k}\sum_{\mu=1}^{\upsilon_{\xi}} g_{\mu,\zeta}^{\xi} b_{\mu}^{\xi} \,(\mathrm{mod}\,2)$ which is then pair by pair or triple by triple mapped to rotated QPSK or 8PSK constellation symbols, respectively, as shown in Figure 2. The coded symbols are then divided into unpunctured and punctured parts. The puncturing process can be described as periodically deleting selected symbols from the output of the encoder in each trellis branch. The puncturing rate defined as the ratio of the number of punctured symbols to total number of symbols at a trellis branch, is chosen according to desired cooperation rate.

In this paper, new cooperative trellis codes with optimized θ^{o} and $g_{\mu,\zeta}^{\xi}$ values are obtained as given in Table 1 by extensive computer search over our design criteria. During the computer search process, the optimum rotation angle and the part of code's generator vector corresponding to the cooperation criterion are obtained by maximizing $\min\{d_{fR_{\min}}^{u}, d_{fI_{\min}}^{u}\}$. Here $d_{fR_{\min}}^{u}$ and $d_{fI_{\min}}^{u}$ denote the minimum values of d_{fR}^{u} and d_{fI}^{u}, respectively. Note that $d_{fR_{\min}}^{u}$ and $d_{fI_{\min}}^{u}$ depend on each other when the same code is used for the two frames between which coordinate interleaving is performed. The remaining part of the generator vector is obtained by maximizing the product $d_{fR}^{u}d_{fI}^{u}d_{fR}^{p}d_{fI}^{p}$. In Table 1, NC1, NC2, and NC3 represent the new 4-, 8-, and 16-state cooperative trellis codes for QPSK, respectively. NC4 and NC5 represent the new 8 and 16-state cooperative trellis codes for 8PSK, respectively. In all of these codes parallel transitions are excluded to avoid their restrictive effect on the error performance. The generic rates of these codes are chosen as 2/4 and 3/6 for QPSK and 8PSK, respectively. The generator vectors are defined as $\mathbf{g}^{\xi} = [(g_{0,1}^{\xi}, g_{0,2}^{\xi}, \ldots, g_{0,n}^{\xi}), (g_{1,1}^{\xi}, g_{1,2}^{\xi}, \ldots, g_{1,n}^{\xi}), \ldots, (g_{\upsilon_{\xi},1}^{\xi}, g_{\upsilon_{\xi},2}^{\xi}, \ldots, g_{\upsilon_{\xi},n}^{\xi})]$, where n is equal to 4 for QPSK and 6 for 8PSK. At each

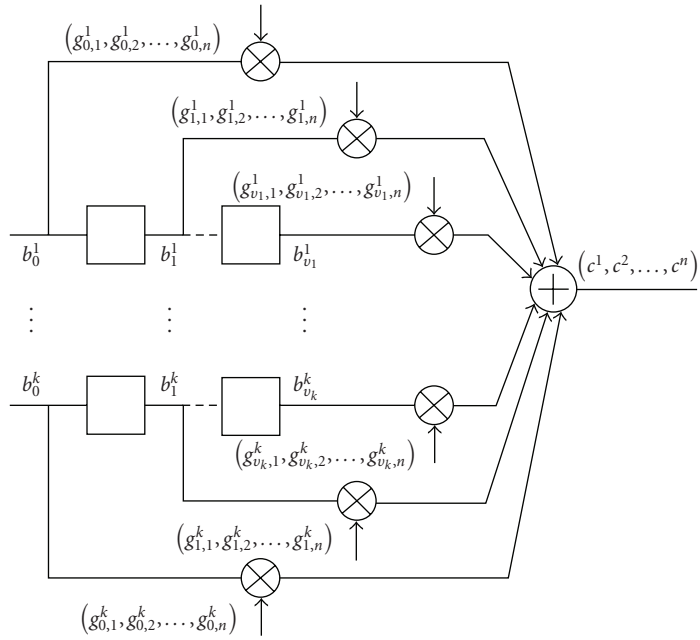

Figure 5: Cooperative trellis encoder.

Table 1: Generator vectors for cooperative trellis codes.

Codes	Modulation	k/n	v	θ^o_{opt}	Generator vectors
NC1	QPSK	2/4	2	19	$\mathbf{g}^1 = [(0101), (1011)]$ $\mathbf{g}^2 = [(1111), (0110)]$
NC2	QPSK	2/4	3	19	$\mathbf{g}^1 = [(1111), (0110)]$ $\mathbf{g}^2 = [(0101), (1010), (1001)]$
NC3	QPSK	2/4	4	19	$\mathbf{g}^1 = [(1111), (0111), (0101)]$ $\mathbf{g}^2 = [(0101), (1001), (1010)]$
NC4	8PSK	3/6	3	9	$\mathbf{g}^1 = [(110110), (101101)]$ $\mathbf{g}^2 = [(011011), (111001)]$ $\mathbf{g}^3 = [(001111), (100010)]$
NC5	8PSK	3/6	4	9	$\mathbf{g}^1 = [(110110), (101111)]$ $\mathbf{g}^2 = [(011111), (111001)]$ $\mathbf{g}^3 = [(001011), (100010), (100010)]$

branch of these cooperative code trellisses, coded bits are mapped to two rotated QPSK or 8PSK symbols, first and second ones forming the unpunctured and punctured symbol sequences, respectively. Thus, all new cooperative trellis codes given in Table 1 have a cooperation rate of 50%.

Best QPSK and 8PSK space-time trellis codes given in [12] for two transmit antennas in slow fading channels are considered as reference codes because of having the same coding rates with the new codes and used in the considered CICC schemes. Optimum rotation angle θ^o is also investigated for these reference codes. The parameters of the new and reference codes for QPSK and 8PSK are shown in Tables 2 and 3, respectively. Here, $CA_{\min}$ and $CC_{\min}$ denote the minimum value of the product $d^u_{fR} d^u_{fI} d^p_{fR} d^p_{fI}$ and $\min\{d^u_{fR_{\min}}, d^u_{fI_{\min}}\}$, respectively.

5. Performance Results

Throughout the performance evaluation by computer simulations, source blocks of 128 and 126 bits including 16 CRC bits with generator polynomial 15935 in hexadecimal form, were considered in each frame for QPSK and 8PSK cooperative codes, respectively. We assumed that all channels are quasistatic, all receivers perfectly know fading coefficients, the destination always knows which cooperation case is realized, and the interuser channel is reciprocal. Moreover, the users were assumed having statistically similar uplink channels. New designed and reference codes with the parameters given in Tables 1, 2, and 3 were considered in the simulations.

First, we assume that no decoding errors occur at the users, and therefore the CICC system always works in the

Table 2: Comparison of new (NC1, NC2, NC3) and reference (V1, V2, V3) QPSK codes.

Codes	υ	θ^o_{opt}	η for C1	$CA_{\min}$	Multiplicity of $CA_{\min}$	$CC_{\min}$	Multiplicity of $CC_{\min}$
NC1	2	19	4	16.786	32	0.769	128
NC2	3	19	4	32.475	704	0.808	64
NC3	4	19	4	74.321	1536	1.153	2048
V1	2	19	4	0.941	32	0.384	64
V2	3	19	4	2.299	64	0.384	256
V3	4	19	4	17.611	256	0.769	1536

Table 3: Comparison of new (NC4, NC5) and reference (V4, V5) 8PSK codes.

Codes	υ	θ^o_{opt}	η for C1	$CA_{\min}$	Multiplicity of $CA_{\min}$	$CC_{\min}$	Multiplicity of CC_{min}
NC4	3	9	4	0.739	3616	0.081	256
NC5	4	9	4	1.153	128	0.096	8192
V4	3	9	4	0.009	256	0.032	512
V5	4	9	4	0.000	556	0.000	556

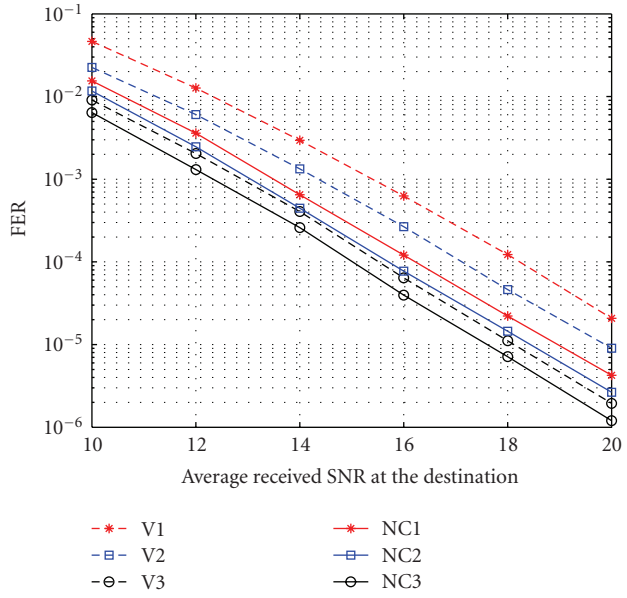

Figure 6: FER performances of QPSK codes for cooperation case C1.

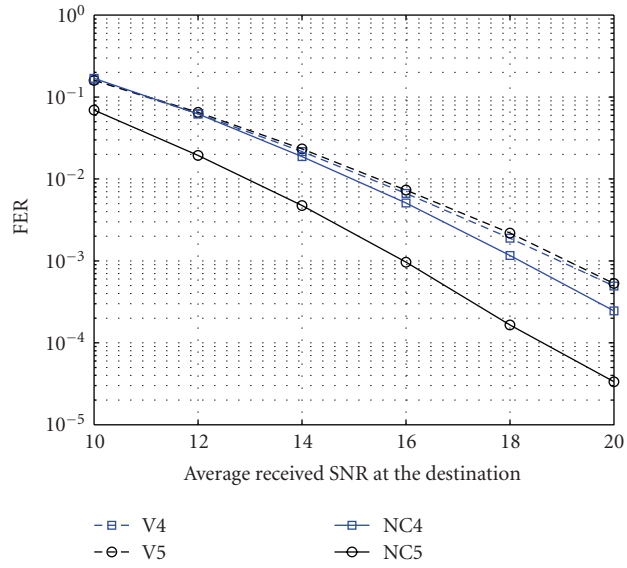

Figure 7: FER performances of 8PSK codes for cooperation case C1.

cooperation case C1. Frame error rate (FER) performance curves under this assumption are given in Figures 6 and 7 for QPSK and 8PSK codes, respectively. These simulation curves are consistent with the $CA_{\min}$ values given in Tables 2 and 3. In Figure 6, 8-state NC2 code which has approximately two times more coding advantage than the 4-state NC1 code provides a received SNR advantage of 0.5 dB at an FER value of 10^{-3}. An additional 0.7 dB received SNR advantage is provided by the 16-state NC3 code which has a good enhancement in $CA_{\min}$ value. At an FER value of 10^{-3}, the received SNR advantages of NC1, NC2, and NC3 over V1, V2, and V3 are 2, 1.4, and 0.5 dB, respectively, as expected from $CA_{\min}$ values of these codes given in Table 2. Also note from these curves that maximum diversity order of four is achieved for all codes. In Figure 7, the 16-state NC5 code which has greater $CA_{\min}$ value and much less multiplicity than the 8-state NC4 code provides a coding advantage of 2 dB at an FER value of 10^{-3}. Both NC4 and NC5 outperform the corresponding reference codes V4 and V5 as expected. Note also that from Figure 7, maximum diversity order of four is achieved for NC4 and NC5 at high SNR values, while diversity orders of V4 and V5 which have approximately zero $CA_{\min}$ values, degrade as expected from the diversity criterion.

Secondly, we consider decoding errors at the users. Differential SNR (dSNR), defined as the difference between

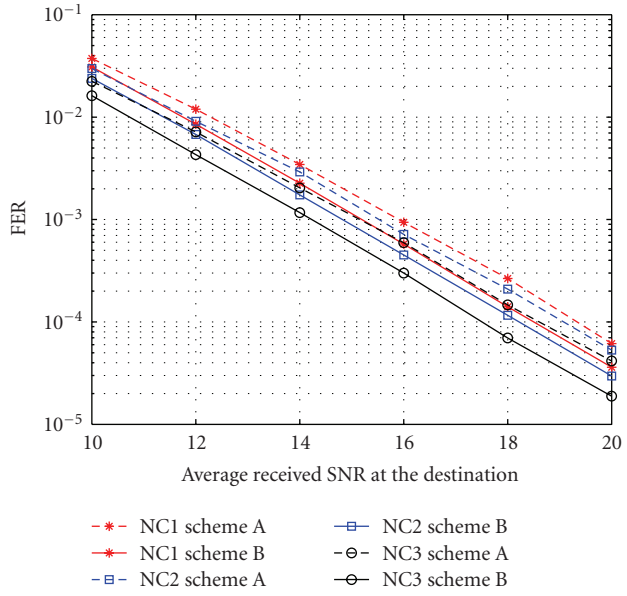

Figure 8: FER performances of new QPSK codes for Schemes A and B (dSNR = 10 dB).

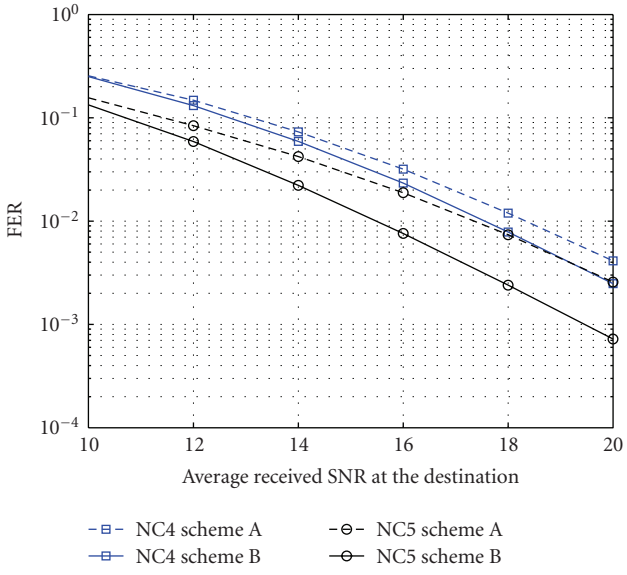

Figure 9: FER performances of new 8PSK codes for Schemes A and B (dSNR = 10 dB).

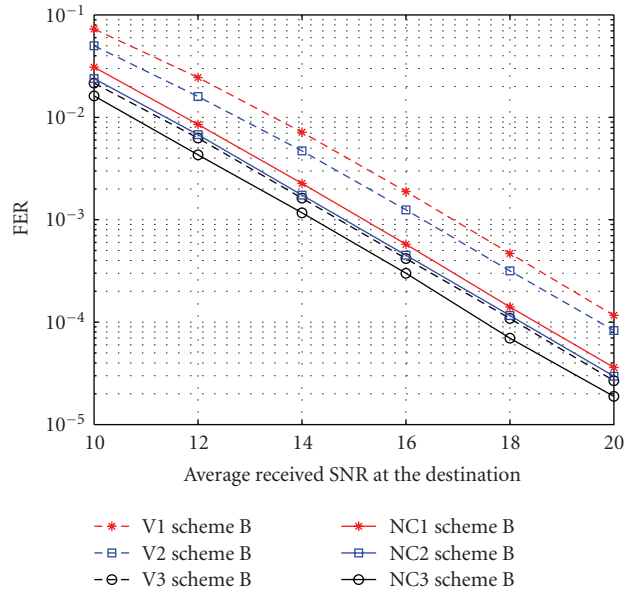

Figure 10: FER performances of QPSK codes for Scheme B (dSNR = 10 dB).

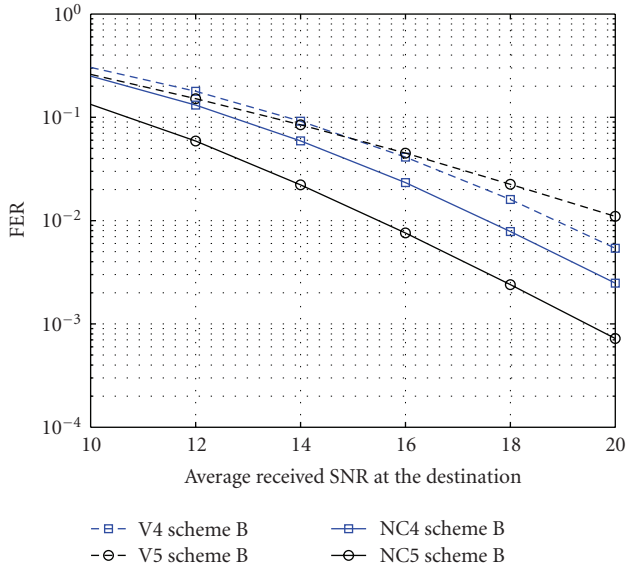

Figure 11: FER performances of 8PSK codes for Scheme B (dSNR = 10 dB).

user-to-destination average received SNR and interuser channel SNR (iSNR), was assumed equal to 10 dB during all simulations. The FER performances of new QPSK and 8PSK codes are compared for CICC Schemes A and B in Figures 8 and 9, respectively. According to Figures 8 and 9, Scheme B provides better performance than Scheme A for all cooperative codes, as expected. In Figure 8, Scheme B provides 0.7, 0.8, and 0.9 dB received SNR advantages compared to Scheme A for NC1, NC2, and NC3 at an FER value of 10^{-3}, respectively. However, for Scheme A, the coding advantage provided by increasing the trellis state number is approximately limited to 0.2 dB while it approaches to 0.5 dB for Scheme B. For Scheme A, the coding advantage provided in C1 with the increase of the trellis states is lost when overall system performance is considered, due to the low FER performance in cases C3 and C4. For 8PSK cooperative codes, from Figure 9, Scheme B provides 0.8 and 1.9 dB received SNR advantages compared to Scheme A for NC4 and NC5 at an FER value of 10^{-2}, respectively. As expected, the coding advantage provided by increasing the trellis state number is 1.0 dB for Scheme A while is increased to 2.0 dB for Scheme B. The FER performances of all QPSK

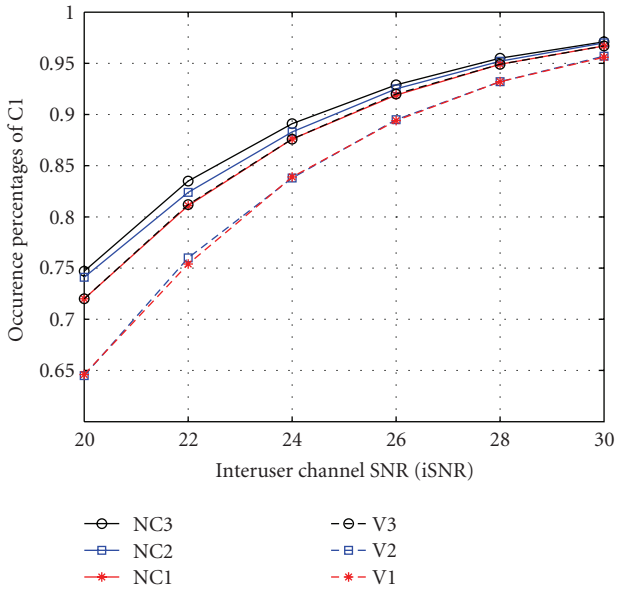

Figure 12: Occurrence percentages of C1 for QPSK codes.

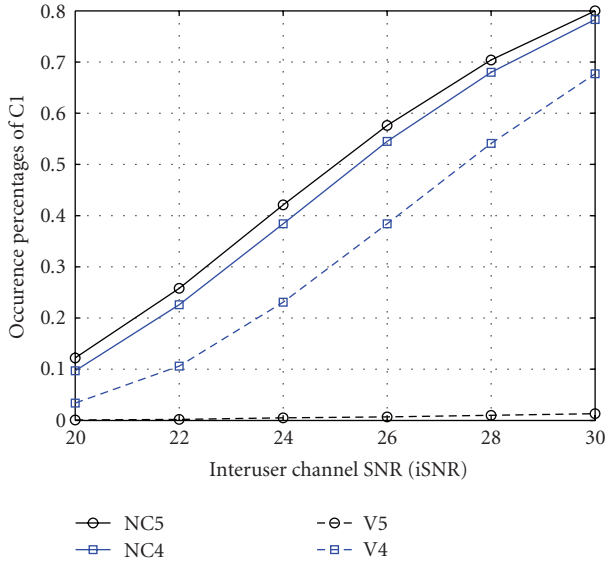

Figure 13: Occurrence percentages of C1 for 8PSK codes.

and 8PSK codes for CICC Schemes B are obtained as given in Figures 10 and 11, respectively. In Figure 10, the received SNR advantages of NC1, NC2, and NC3 over V1, V2, and V3 are 1.8, 1.6, and 0.5 dB at an FER value of 10^{-3}, respectively. Both NC4 and NC5 outperform the corresponding reference codes V4 and V5 as seen in Figure 11. At an FER value of 10^{-2}, NC4 and NC5 have 1.4 and 4.5 dB received SNR advantages over V4 and V5. Occurrence percentages of the cooperation case C1 for QPSK and 8PSK codes are given in Figures 12 and 13, respectively, for iSNR values changing from 20 to 30 dB. These simulation curves are fully consistent with the $CC_{\min}$ values given in Tables 2 and 3. Note that from these curves, occurence percentage of C1 increases with increasing values of $CC_{\min}$.

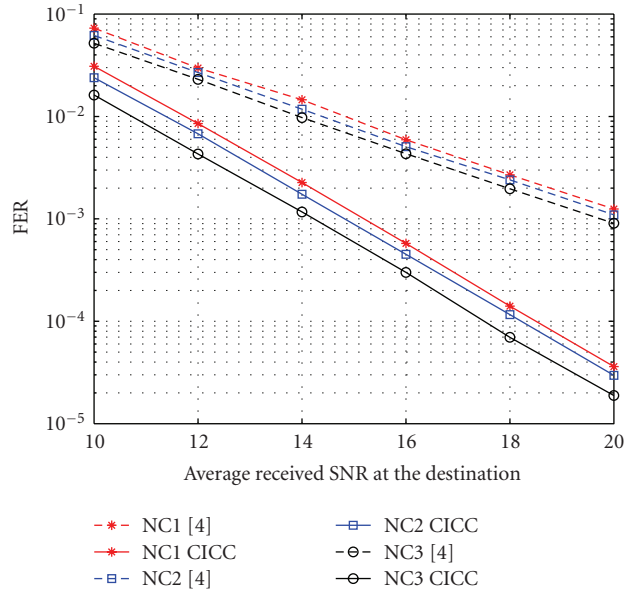

Figure 14: Performance comparison of the proposed QPSK codes for classical [4] and CI coded cooperation.

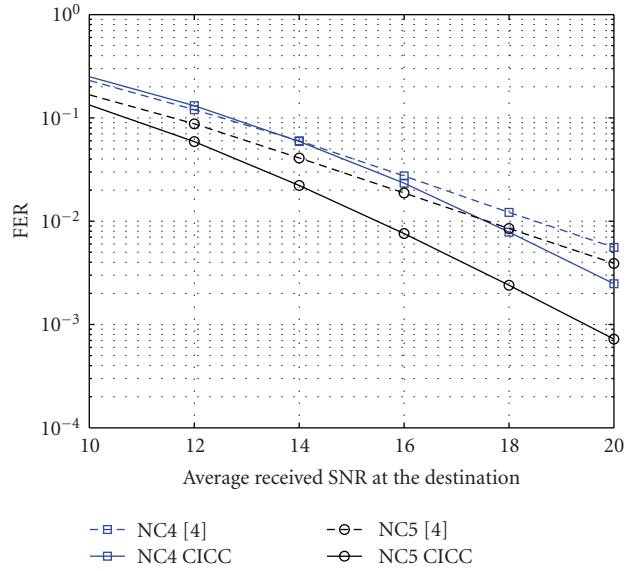

Figure 15: Performance comparison of the proposed 8PSK codes for classical [4] and CI coded cooperation.

Finally, we compare performances of the proposed QPSK and 8PSK codes for classical [4] and CI coded cooperation in Figures 14 and 15, respectively. It is obvious that the proposed CICC technique reaches maximum diversity order of four at high SNR values while classical one has maximum diversity order of two. Due to the diversity gain, proposed CICC technique provides approximately 5.5 dB received SNR advantage against classical one for all QPSK codes (NC1, NC2, and NC3) at an FER value of 10^{-3}. For 8PSK codes (NC4 and NC5), the received SNR advantages of CICC over classical one are 1 and 2 dB at an FER value of 10^{-2},

respectively. Since occurrence percentages of the cooperation case C1 for 8PSK codes are not as much as for QPSK codes, 8PSK codes exhibit lower diversity order and therefore lower received SNR advantage than QPSK codes for the considered SNR ranges.

6. Conclusion

In this paper, a two-user cooperative communication scheme, which combines coded cooperation and modulation diversity techniques, has been proposed for wireless communication systems. Two times more diversity has been achieved compared to the pure coded cooperation scheme, due to the fact that the proposed system takes full advantage of both the cooperation and modulation diversities. New code design criteria have been derived for CICC systems, and cooperative trellis codes for QPSK and 8PSK have been obtained by exhaustive computer search. The new codes have better error performance than the corresponding best space-time codes used in cooperation with CI, which shows that the best space-time trellis codes given in literature are not the best codes for the CICC systems.

Appendix

Proof of Theorem 1. For (2), maximum likelihood (ML) detection metric can be written as

$$\left|\mathbf{r}_{1,1}^{(12)} - h_{1,12}\left(\mathbf{x}_{1R}^{(1)u} + j\mathbf{x}_{2I}^{(1)u}\right)\right|^2. \tag{A.1}$$

By deleting the terms which are independent of $\mathbf{x}_{1R}^{(1)u}$ and $\mathbf{x}_{2I}^{(1)u}$, (A.1) can be rewritten as

$$\begin{aligned}&|h_{1,12}|^2\left(\left|\mathbf{x}_{1R}^{(1)u}\right|^2 + \left|\mathbf{x}_{2I}^{(1)u}\right|^2\right)\\ &\quad - h_{1,12}\left(\mathbf{x}_{1R}^{(1)u} + j\mathbf{x}_{2I}^{(1)u}\right)\left(\mathbf{r}_{1,1}^{(12)}\right)^* - \mathbf{r}_{1,1}^{(12)}h_{1,12}^*\left(\mathbf{x}_{1R}^{(1)u} - j\mathbf{x}_{2I}^{(1)u}\right)^T,\end{aligned} \tag{A.2}$$

which can be decomposed into two parts, where

$$|h_{1,12}|^2\left|\mathbf{x}_{1R}^{(1)u}\right|^2 - h_{1,12}\mathbf{x}_{1R}^{(1)u}\left(\mathbf{r}_{1,1}^{(12)}\right)^* - \mathbf{r}_{1,1}^{(12)}h_{1,12}^*\left(\mathbf{x}_{1R}^{(1)u}\right)^T \tag{A.3}$$

is only function of $\mathbf{x}_{1R}^{(1)u}$, and

$$|h_{1,12}|^2\left|\mathbf{x}_{2I}^{(1)u}\right|^2 - jh_{1,12}\mathbf{x}_{2I}^{(1)u}\left(\mathbf{r}_{1,1}^{(12)}\right)^* + j\mathbf{r}_{1,1}^{(12)}h_{1,12}^*\left(\mathbf{x}_{2I}^{(1)u}\right)^T \tag{A.4}$$

is only function of $\mathbf{x}_{2I}^{(1)u}$. Equations (A.3) and (A.4) can be finally modified as

$$\left|\mathbf{r}_{1,1}^{(12)} - h_{1,12}\mathbf{x}_{1R}^{(1)u}\right|^2, \tag{A.5}$$

$$\left|\mathbf{r}_{1,1}^{(12)} - jh_{1,12}\mathbf{x}_{2I}^{(1)u}\right|^2, \tag{A.6}$$

respectively, since $|\mathbf{r}_{1,1}^{(12)}|^2$ is independent of $\mathbf{x}_{1R}^{(1)u}$ and $\mathbf{x}_{2I}^{(1)u}$. Therefore, to minimize (A.1) we can minimize (A.5) and (A.6) separately for detecting $\mathbf{x}_{1R}^{(1)u}$ and $\mathbf{x}_{2I}^{(1)u}$, respectively. These are simple and unique decoding metrics which can be used without deinterleaving process at the receiver side. □

Acknowledgment

This work was supported by the Scientific and Technological Research Council of Turkey TUBITAK, Project no. 107E022.

References

[1] A. Sendonaris, E. Erkip, and B. Aazhang, "Increasing uplink capacity via user cooperation diversity," in *Proceedings of IEEE International Symposium on Information Theory*, p. 156, Cambridge, Mass, USA, August 1998.

[2] J. N. Laneman, *Cooperative diversity in wireless networks: algorithms and architectures*, Ph.D. thesis, Massachusetts Institute of Technology, Cambridge, Mass, USA, 2002.

[3] T. E. Hunter and A. Nosratinia, "Coded cooperation under slow fading, fast fading, and power control," in *Proceedings of the 36th Asilomar Conference on Signals, Systems and Computers*, vol. 1, pp. 118–122, November 2002.

[4] T. E. Hunter and A. Nosratinia, "Diversity through coded cooperation," *IEEE Transactions on Wireless Communications*, vol. 5, no. 2, pp. 283–289, 2006.

[5] K. Ho-Van and T. Le-Ngoc, "A bandwidth-efficient coded user-cooperation scheme for flat block fading channels," in *Proceedings of the 4th IEEE Internatilonal Symposium on Wireless Communication Systems (ISWCS '07)*, pp. 421–425, October 2007.

[6] J. Li and A. Stefanov, "Cooperative multiple trellis coded modulation," in *Proceedings of IEEE Military Communications Conference (MILCOM '06)*, pp. 1–6, Washington, DC, USA, October 2006.

[7] J. Li and A. Stefanov, "General design criteria and properties of cooperative MTCM systems," in *Proceedings of IEEE Global Telecommunications Conference (GLOBECOM '07)*, pp. 3432–3436, November 2007.

[8] G. Taricco and E. Viterbo, "Performance of component interleaved signal sets for fading channels," *Electronics Letters*, vol. 32, no. 13, pp. 1170–1172, 1996.

[9] J. Boutros and E. Viterbo, "Signal space diversity: a power- and bandwidth-efficient diversity technique for the Rayleigh fading channel," *IEEE Transactions on Information Theory*, vol. 44, no. 4, pp. 1453–1467, 1998.

[10] M. Z. A. Khan and B. S. Rajan, "Single-symbol maximum likelihood decodable linear STBCs," *IEEE Transactions on Information Theory*, vol. 52, no. 5, pp. 2062–2091, 2006.

[11] J. Harshan and B. S. Rajan, "Coordinate interleaved distributed space-time coding for two-antenna-relays networks," in *Proceedings of IEEE Global Telecommunications Conference (GLOBECOM '07)*, pp. 1719–1723, November 2007.

[12] B. Vucetic and H. Yuan, *Space-Time Coding*, John Wiley & Sons, New York, NY, USA, 2003.